Aminolipid biosynthesis in response to phosphate limitation promotes colistin tolerance in *Acinetobacter baumannii*

Roberto Jhonatan Olea-Ozuna[1], Melanie J. Campbell[2], Samantha Y. Quintanilla[1], Sinjini Nandy[1], Jennifer S. Brodbelt[2], and Joseph M. Boll[1, #]

Affiliations:

[1]Department of Biological Sciences, University of Texas at Dallas, Richardson, TX, USA

[2]Department of Chemistry, University of Texas at Austin, Austin, TX, USA

[#]Correspondence:

Joseph M. Boll

The University of Texas at Dallas

Phone (972) 883-6529

Email: joseph.boll@utdallas.edu

Running Head: Aminolipid synthesis in *Ab* under phosphate limitation

Keywords: aminolipids, ornithine lipids, lysine lipids, phosphate, colistin

Abstract

The Gram-negative outer membrane protects bacterial cells from environmental toxins such as antibiotics. The outer membrane lipid bilayer is asymmetric; while glycerophospholipids compose the periplasmic facing leaflet, the surface layer is enriched with phosphate-containing lipopolysaccharides. The anionic phosphates that decorate the cell surface promote electrostatic interactions with cationic antimicrobial peptides such as colistin, allowing them to penetrate the bilayer, form pores, and lyse the cell. Colistin is prescribed as a last-line therapy to treat multidrug-resistant Gram-negative infections.

Acinetobacter baumannii is an ESKAPE pathogen that rapidly develops resistance to antibiotics and persists for extended periods in the host or on abiotic surfaces. Survival in environmental stress such as phosphate scarcity, represents a clinically significant challenge for nosocomial pathogens. In the face of phosphate starvation, certain bacteria encode adaptive strategies, including the substitution of glycerophospholipids with phosphorus-free lipids. In bacteria, phosphatidylethanolamine, phosphatidylglycerol, and cardiolipin are conserved glycerophospholipids that form lipid bilayers. Here, we demonstrate that in response to phosphate limitation, conserved regulatory mechanisms induce aminolipid production in *A. baumannii*. Specifically, phosphate limitation induces formation of three lipids, including amine-containing ornithine and lysine aminolipids. Mutations that inactivate aminolipid biosynthesis exhibit fitness defects relative to wild type in colistin growth and killing assays. Furthermore, we show that other Gram-negative ESKAPE pathogens accumulate aminolipids under phosphate limiting growth conditions, suggesting aminolipid biosynthesis may represent a broad strategy to overcome cationic antimicrobial peptide-mediated killing.

49 **Importance**

50 Gram-negative ESKAPE pathogens, including A*cinetobacter baumannii*, are
51 responsible for a dramatic increase in the morbidity and mortality of patients in healthcare
52 settings over the past two decades. Infections are difficult to treat due to antibiotic resistance
53 and tolerance; however, broadly conserved mechanisms that promote antibiotic treatment
54 failure have not been extensively studied. Herein, we identify an alternative lipid biosynthesis
55 pathway that is induced in phosphate starvation that enables Gram-negative ESKAPE
56 pathogens, including *A. baumannii*, *Klebsiella pneumoniae*, and *Enterobacter cloacae* to
57 build lipid bilayers in the absence of glycerophospholipids, which are the canonical lipids.
58 Replacement of the anionic phosphate in the lipid headgroup with zwitterionic ornithine and
59 lysine promote survival against colistin, a last resort antimicrobial used against Gram-
60 negative infections. These studies suggest that ESKAPE pathogens can remodel their bilayers
61 with phosphate free lipids to overcome colistin treatment and that aminolipid biosynthesis
62 could be targeted to improve antimicrobial treatment.
63
64
65
66
67
68
69
70
71
72

Introduction

The Gram-negative cell envelope consists of a symmetrical bilayer of glycerophospholipids in the inner membrane, while the outer membrane exhibits an asymmetrical composition, with glycerophospholipids in the periplasmic leaflet and lipopolysaccharide enriched in the outer leaflet (1). The intricate organization underscores the remarkable complexity of bacterial membrane architecture, crucial for microbial survival in various environments. However, under specific stress conditions such as nutrient limitation, temperature fluctuations or exposure to antimicrobial agents, certain bacteria activate alternative lipid biosynthesis pathways or modify existing lipids to adapt and ensure cellular viability (2). One example is aminolipids, which contain amino acid headgroups like lysine, glycine, glutamine, and serine-glycine, with ornithine being the most common (3, 4). Ornithine lipids (OLs) are phosphorus-free and found exclusively in bacteria; they are absent in archaea or eukaryotes (5). Their basic structure comprises a 3-hydroxylated fatty acid linked by an amide bond to the α-amino group of ornithine and a second fatty acid attached by an ester bond to the 3-hydroxyl group of the first fatty acid (6). Although OLs are found in both the inner and outer lipid bilayers of Gram-negative bacteria, they are enriched in the outer membrane (7–10). OL biosynthesis is catalyzed by two acyltransferases, OlsB and OlsA, or by the bifunctional acyltransferase OlsF (11–13). In some Gram-negative pathogens such as *Pseudomonas aeruginosa* or *Vibrio cholerae*, OLs are exclusively formed under phosphate limiting conditions (14, 15), indicating the presence of a specific regulatory mechanism. The importance of aminolipids transcends basic physiology, especially in the context of antibiotic resistance. ESKAPE pathogens, a group of pathogens that include *Acinetobacter baumannii*, are notorious for their ability to overcome antibiotic treatment and cause hospital-acquired infections (16). Aminolipid synthesis has been implicated in

97 increased bacterial fitness under antimicrobial stress (9, 17, 18), potentially contributing to
98 pathogen persistence in clinical settings. Additionally, there is a notable relationship between
99 membrane lipid remodeling and resistance to colistin, a last-resort antibiotic that is used
100 against multi-drug resistant Gram-negative infections (19–22). Chemical modifications to
101 the lipid A domain of lipopolysaccharide or enrichment of amino acid-containing
102 glycerophospholipids have been associated with colistin resistance (23–25), highlighting the
103 importance of understanding lipid metabolism in combating antibiotic resistance.

104 In this study, we demonstrate that *A. baumannii* produced two aminolipids in limiting
105 phosphate growth conditions, including lysine lipids (LLs) and OLs. OL and LL synthesis is
106 dependent on the *olsB* and *olsA* genes, and *olsB* expression is regulated transcriptionally by
107 the response regulator, PhoR. Additionally, mutants deficient in aminolipid synthesis exhibit
108 increased colistin susceptibility relative to wild type. We also found that other Gram-negative
109 ESKAPE pathogens, including *Klebsiella pneumoniae* and *Enterobacter cloacae*,
110 accumulate aminolipids under phosphate limited growth conditions. These findings suggest
111 a broad survival strategy among ESKAPE pathogens that could promote survival during
112 antibiotic treatment.
113
114
115
116
117
118
119
120

121 **Results**

122 **Phosphate limitation induces lipid membrane composition modifications in *A.***
123 ***baumannii***

124 The membrane lipid composition of diverse *A. baumannii* isolates was analyzed,
125 including strains ATCC 17978, ATCC 19606, and AB5075, cultivated in complex lysogeny
126 broth (LB) medium supplemented with ^{32}P-orthophosphoric acid. Labelled cells were
127 collected at mid-logarithmic growth phase, lipids were extracted using the Bligh and Dyer
128 method, and separated by hydrophobicity using two-dimensional thin-layer chromatography
129 (TLC), as previously done (26). We also prepared lipid extracts from well-characterized
130 *Escherichia coli* K-12 strain W3110 for comparison (27). TLC analysis showed conserved
131 glycerophospholipid enrichment corresponding to known structures, including
132 phosphatidylethanolamine (PE), phosphatidylglycerol (PG), and cardiolipin (CL) (**Figure**
133 **S1A**). Additionally, *A. baumannii* strains also produced two distinct lipid species, including
134 lyso-PE (20) and an unknown phospholipid, denoted as UPL1, that could be a CL derivative,
135 mono-lyso CL (28). The chemical structures of known phospholipids are shown in **Figure**
136 **S1B**.

137 *A. baumannii* strain ATCC 17978 cultured in minimal medium with 1 mM (excess)
138 phosphate displayed a lipid composition almost equivalent to growth in complex LB medium
139 (**Figure 1 and Figure S1A**). One notable change was that UPL1 was absent, and another
140 unidentified lipid, denoted as UPL2, was formed, likely representing another CL derivative.
141 To explore lipid biosynthesis under phosphate-limiting condition, membrane lipid profiles
142 were analyzed after growth in minimal media supplemented with 50 μM (limiting) phosphate
143 concentrations (**Figure 1**). Limited phosphate availability impacted relative lipid levels,
144 suggesting decreased phosphate-containing lipid synthesis. Concomitant production of three

145 unknown lipids, referred to as unknown lipids 1 (U1), 2 (U2), and 3 (U3), were produced in
146 phosphate limiting growth. Ninhydrin staining revealed that U1 and U2 contained free
147 amines, like PE. Increased ratios of ninhydrin-stained unknown aminolipids relative to PE
148 showed that under phosphate-limiting conditions, potential phosphate-free aminolipids were
149 produced.

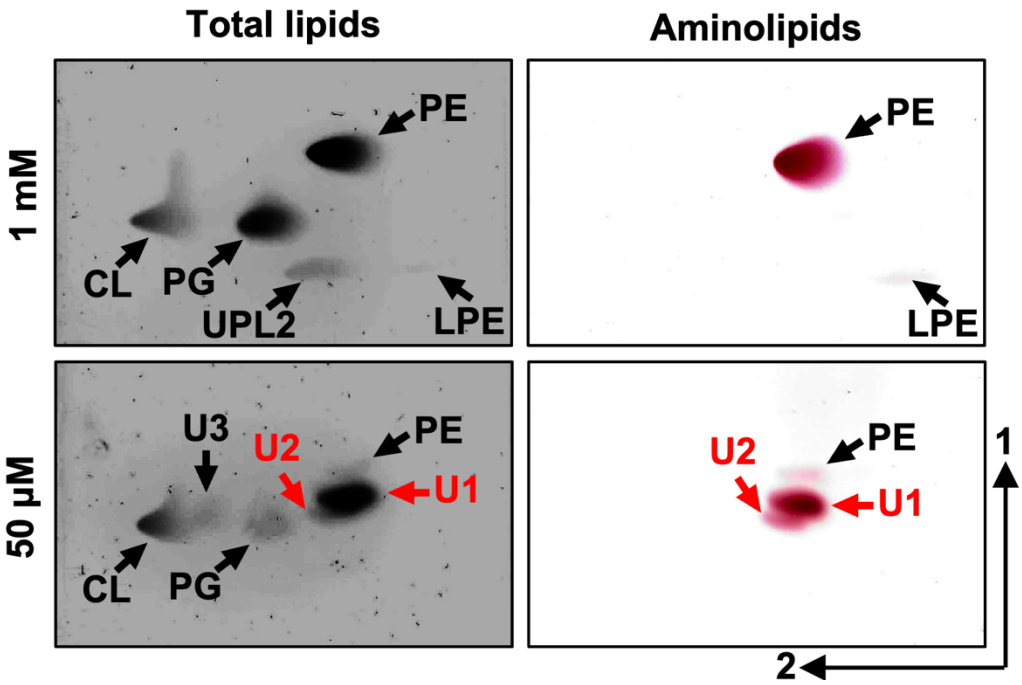

Figure 1: Lipid composition of *A. baumannii* strain ATCC 17978 in excess and limiting phosphate concentrations. Strains were grown in minimal with excess (1 mM) or limiting (50 µM) phosphate. Cells were collected, lipids were extracted using the Bligh and Dyer method and separated using 2-dimensional thin-layer chromatography. Total lipids were stained with sulfuric acid (left). Aminolipids were stained using ninhydrin (right). Specific lipids are labelled: PE, phosphatidylethanolamine; PG, phosphatidylglycerol; CL, cardiolipin; LPE, lyso-PE; U1, unknown lipid 1; U2, unknown lipid 2; U3, unknown lipid 3; UPL2, unknown phospholipid 2. Red letters denote aminolipids that provide the focus of the study.

158 Growth in limiting phosphate concentrations slowed growth in ATCC 17978 relative
159 to excess phosphate (**Figure S2A**), and microscopic analysis revealed that cells elongated
160 and increased their surface area when phosphate is limiting (**Figure S2B and S2C**), a
161 response previously reported in other Gram-negative bacteria (29). Additionally, while the
162 composition of lipooligosaccharide (LOS) fractions remained consistent across limiting

163 phosphate conditions, the relative level of LOS was decreased under phosphate limitation
164 (**Figure S2D**).
165
166 **Aminolipids synthesized during phosphate limitation are OLs and LLs**
167 One dimensional TLC showed three lipids (PE, U1, and U2) stained with ninhydrin
168 (**Figure S3A**). After separation of lipids based on hydrophobicity, individual bands
169 corresponding with U1 and U2 were scraped from the TLC plates and extracted using the
170 Bligh and Dyer method. U1 and U2 bands were analyzed by liquid-chromatography mass
171 spectrometry (LC-MS) and structurally characterized using tandem mass spectrometry
172 (MS/MS) (**Figure 2**). The elution profiles obtained for the U1 and U2 bands are displayed in
173 **Figures 2A** and **2D,** respectively. To determine the composition of aminolipids, a data-
174 dependent acquisition method was used to isolate and activate the most abundant ions
175 detected in each chromatographic peak with higher energy collisional dissociation (HCD) in
176 negative-ionization mode. HCD of precursor *m/z* 621.52 found in the U1 extract resulted in
177 the loss of the headgroup, which was observed at *m/z* 131.08, and corresponded to
178 deprotonated ornithine (**Figure 2B**). The most abundant fragment ion (*m/z* 367.30) was used
179 to identify the acyl chain connected to the headgroup as 16:0 (number of carbon atoms:
180 double bonds). Further, the complementary ion of *m/z* 253.22 confirmed the identity of the
181 fatty acid connected at the 3-hydroxyl position of the first fatty acid as 16:1. Following this
182 analysis, lipids containing a double bond were subsequently targeted in second LC run in the
183 positive-ionization mode using 193 nm ultraviolet photodissociation (UVPD) for MS/MS.
184 UVPD is an alternative fragmentation method that utilizes high-energy photons to activate
185 and dissociate the selected lipid precursor ions, allowing localization of the double bonds
186 within the fatty acyl chains. UVPD of precursor *m/z* 623.53 produced two fragment ions

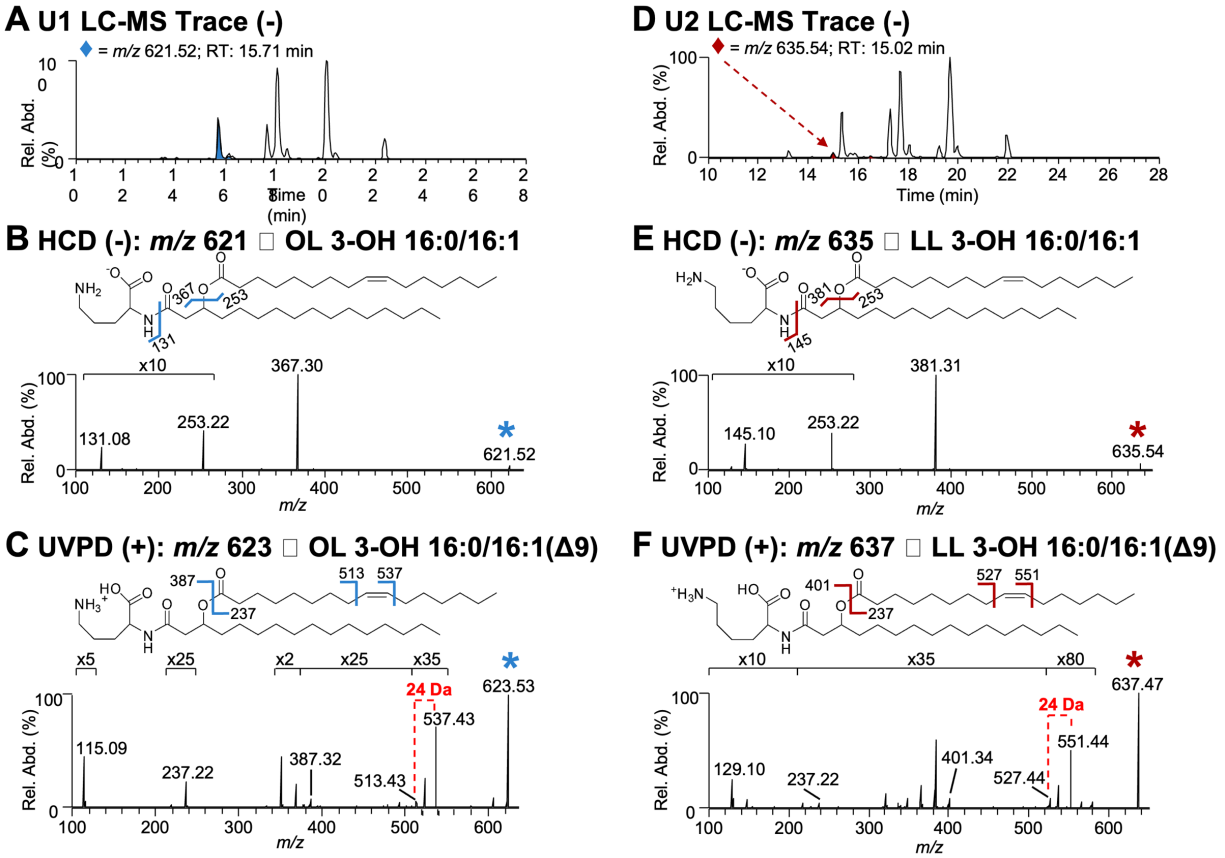

Figure 2: Structural analysis of the lipids produced during phosphate limitation. A. LC-MS trace of U1 lipid extract in negative ionization mode. **B.** HCD (NCE 22) mass spectrum of *m/z* 621.52 ($[M-H]^-$), an ornithine lipid found in U1 extract**. C.** UVPD (4 pulses at 2 mJ/pulse) mass spectrum of *m/z* 623.53 ($[M+H]^+$). **D.** LC-MS trace of U2 lipid extract in negative ionization mode. **E.** HCD (NCE 22) mass spectrum of *m/z* 635.54 ($[M-H]^-$), a lysine lipid found in U2 extract. **F.** UVPD (4 pulses at 2 mJ/pulse) mass spectrum of *m/z* 637.47 ($[M+H]^+$). The selected precursor ions are labeled with asterisks in B,C,E, and F.

separated by 24 Da that originate from cleavages adjacent to the double bond. This pair of diagnostic ions localizes the double bond to the 9th position (**Figure 2C**). This LC-MS/MS strategy identified 49 OLs, including double bond isomers, and 10 unknown lipids in the U1 extract (**Table S1**) and a total of 24 OLs and 16 unknown lipids in the U2 extract (**Table S2**). HCD of the unknown lipids yielded similar fragmentation to that observed for OLs, but the fragmentation patterns were distinguished by the release of a deprotonated headgroup that corresponded to either a lysine or monomethylated ornithine headgroup (*m/z* 145.10) (**Figure 2E**). While the aminolipid head group could be either lysine or monomethylated ornithine,

195 the absence of an ortholog for OlsG, the enzyme responsible for OL methylation (30), and
196 the presence of *olsG* only in certain planctomycete genomes, strongly suggests that OL
197 methylation is unlikely to occur in *A. baumannii*. Therefore, the identified lipid is denoted
198 herein as a LL.

199 After confirming that *A. baumannii* strain ATCC 17978 produces OLs and LLs, we
200 explored if other *A. baumannii* isolates form these aminolipids during phosphate limitation.
201 One-dimensional TLC stained with ninhydrin revealed that diverse *A. baumannii* strains,
202 including ATCC 17978, ATCC 19606, AB5075, AYE, and the environmental isolate, *A.*
203 *baylyi*, were also capable of aminolipid biosynthesis in response to phosphate limitation
204 (**Figure S3B**). Together, these studies suggest that *Acinetobacter* can form lipid bilayers with
205 not only glycerophospholipids, but also membranes enriched with OLs and LLs when
206 phosphate availability is limited.

207

208 **Differentially regulated genes during phosphate starvation**

209 To determine genes that regulate aminolipid biosynthesis, total RNA was isolated,
210 rRNA was depleted, and transcripts were sequenced from *A. baumannii* strain ATCC 17978
211 after growth in minimal media supplemented with 1 mM (excess) and 50 μM (limiting)
212 phosphate. Using a cutoff of 3-fold weighted proportions fold change with an FDR p-
213 value correction < 0.05, 67 upregulated genes and 109 downregulated genes were found
214 (**Figure 3A**). Many down-regulated genes were involved in iron uptake and lysine
215 degradation. Upregulated genes included pathways involved in TAT-dependent proteins
216 export, phospholipases, lipid metabolism, regulation and phosphate transporters. A complete
217 list of significant ($P < 0.05$) up- and down-regulated genes is included in **Table S3**.

218 One notable up-regulated gene (*A1S_0889*) showed 31% identity and 51% similarity
219 (91% coverage) to *P. aeruginosa olsB*. While not induced in phosphate starvation, *A.*
220 *baumannii* also encodes a putative *olsA* orthologue (*A1S_2990*) with 43% identity and 61%
221 similarity (78% coverage) to *P. aeruginosa olsA*. OlsBA has been characterized in several
222 bacteria and is involved in OLs biosynthesis (8, 11, 12, 14, 31). Notably, *A. baumannii olsA*

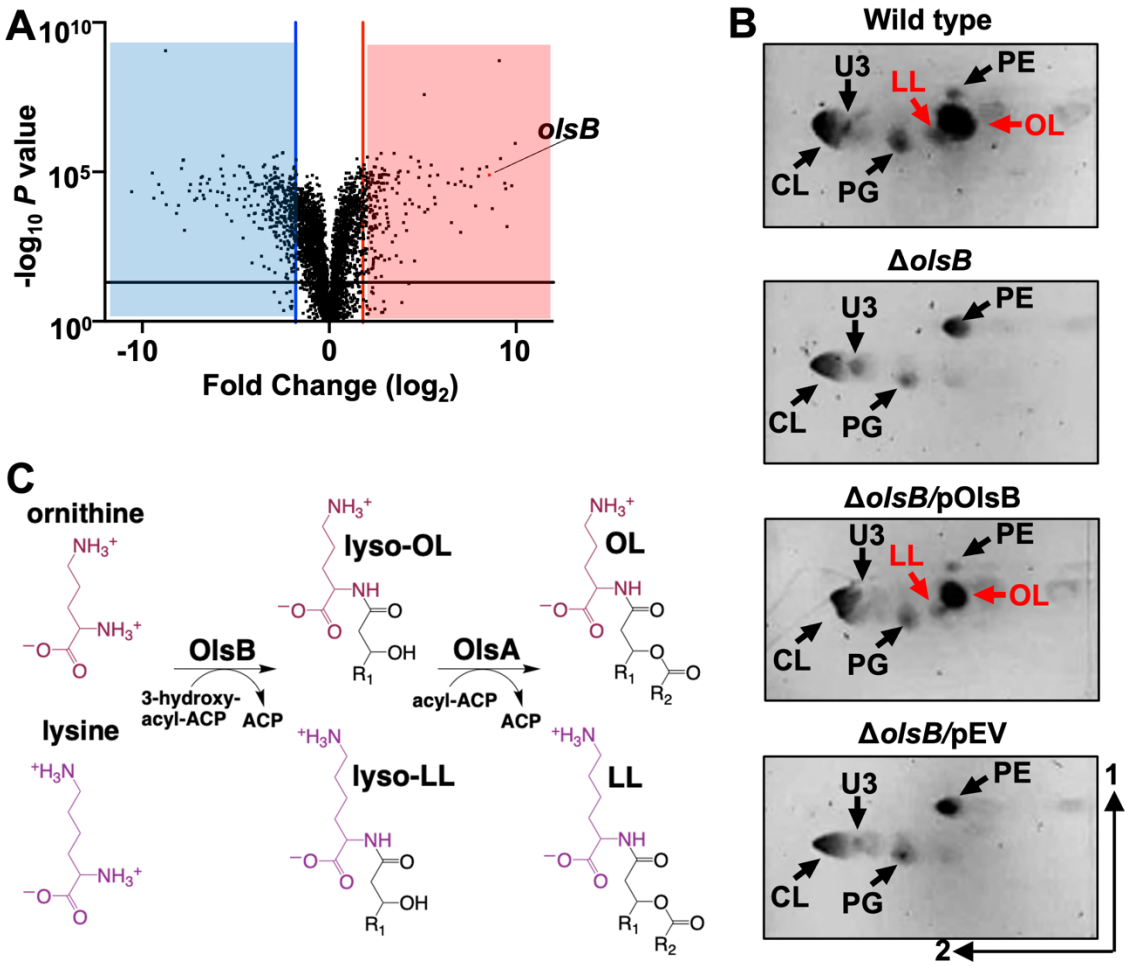

Figure 3: The *olsB* gene is required for ornithine and lysine lipid formation in phosphate limited growth conditions. A. Volcano plot of differentially regulated genes in excess and limiting phosphate. Red/blue lines indicate 3-fold cutoffs. The Black line on the *x*-axis indicates $P < 0.05$. A red dot representing the *olsB* expression profile is shown. **B.** 2D thin-layer chromatography stained with sulfuric acid showing wild type and Δ*olsB* strains grown in phosphate limiting (50 µM) conditions. Specific lipids are labelled: PE, phosphatidylethanolamine; PG, phosphatidylglycerol; CL, cardiolipin; OL, ornithine lipid; LL, lysine lipid; U3, unknown lipid 3. OL and LL aminolipids are labelled in red. **C.** Proposed ornithine lipid (OL) and lysine lipid (LL) biosynthesis pathways in *A. baumannii*.

223 is located at a distinct site on the chromosome relative to *olsB* and is not transcriptionally
224 regulated by phosphate concentrations.
225
226 ***olsB* and *olsA* genes are required for aminolipids synthesis in *A. baumannii***
227 Differential gene expression analysis indicated changes in gene dosage in response to
228 excess/limiting phosphate concentration. Specifically, *A1S_0889* expression increased in
229 response to phosphate limitation, whereas *A1S_2990* expression did not change. To confirm
230 that *A1S_0889* was an *olsB* orthologue, we generated Δ*olsB* in *A. baumannii* strain ATCC
231 17978, by fusing codon 33 and 215. TLC analysis revealed that under phosphate limitation,
232 aminolipids were absent in the *olsB*-deficient mutant and a mutant carrying only the empty
233 vector but wild-type accumulated OLs and LLs (**Figure 3B**). Furthermore, *olsB*
234 complementation from a non-native promoter restored OL and LL formation. Based on the
235 lipid migration patterns in wild type, the lipids are OLs and LLs.
236 Additionally, we generated Δ*olsB* (HMPREF0010_01383) in strain ATCC 19606 and
237 analyzed the *olsB::tn* and *olsA::tn* mutants for the AB5075 transposon mutant library (32) in
238 the respective genes, ABUW_3039 and ABUW_0502. Lipid analysis when the mutants were
239 cultivated under phosphate limitation showed that the wild-type strains ATCC 19606 and
240 AB5075 produced OLs and LLs, while the *olsB* and *olsA* mutants did not (**Figure S4A and**
241 **S4B**). The *olsA*::*tn* mutant lipid profile did not show the expected accumulation of lyso-
242 aminolipids, consistent with findings in other Gram-negative Δ*olsA* mutants (33). This
243 suggests that lyso-aminolipids are tightly regulated and rapidly degraded within the cell.
244 These data suggested that ornithine and lysine lipid biosynthesis in *A. baumannii* is
245 dependent on OlsB and OlsA.

246 Together, this data supports a model suggesting that aminolipid synthesis occurs in at
247 least two distinct steps within *A. baumannii* (**Figure 3C**). Initially, ornithine and lysine
248 undergo acylation in an OlsB-dependent reaction, leading to the formation of lyso-OL and
249 lyso-LL. Subsequently, in a second step facilitated by OlsA, lyso-OL and lyso-LL are further
250 acylated at the hydroxy position, yielding OL and LL, respectively.

251 Microscopic analysis and comparison of LOS fractions and levels between
252 aminolipid-producing and aminolipid-deficient *A. baumannii* strains revealed no significant
253 morphological differences (**Figure S4C and S4D**) or changes in LOS fractions and relative
254 levels (**Figure S2D)**. However, it is noteworthy that the core fraction of LOS from *A.*
255 *baumannii* strains ATCC 19606 differs from of the ATCC 17978 or AB5075 strains.
256 Additionally, a faint band in the core fraction was observed in the *olsA*::*tn* transposon mutant
257 of AB5075, which was not present in the wild type strain.

258

259 **Mutants deficient in aminolipids synthesis show differential growth rate under**
260 **phosphate limitation**

261 To assess growth rates under phosphate limitation, wild-type and *olsB* mutant strains
262 were grown in minimal medium with limiting phosphate concentrations (**Figure S4E**). The
263 optical density at 600 nm (OD_{600}) was monitored over time. While growth of strain ATCC
264 17978 Δ*olsB* was not impacted, the growth rate in strains ATCC 19606 and AB5075 was
265 reduced in the *olsB* or *olsA* Tn*101*mutants, suggesting there are strain-dependent effects on
266 aminolipid biosynthesis that impact fitness.

267

268 **Aminolipid biosynthesis mutants are defective in colistin tolerance**

269 Changes in lipid composition could alter the physicochemical properties of the
270 bilayers, particularly the charge. To explore this concept, the impact of aminolipids
271 biosynthesis on colistin tolerance was measured in *A. baumannii* strain ATCC 17978, where
272 growth rate was not impacted in the *olsB* mutant (**Figure S4E**). Colistin is a cyclic peptide
273 that directly engages with the negative membrane charge, while the hydrophobic tail forms
274 pores, leading to bactericidal activity. Colistin is a last resort antibiotic used against multidrug
275 resistant Gram-negative bacterial infections. Our studies indicate increased colistin
276 susceptibility in the *olsB*-deficient mutant relative to the wild-type strain (**Figure 4A and**

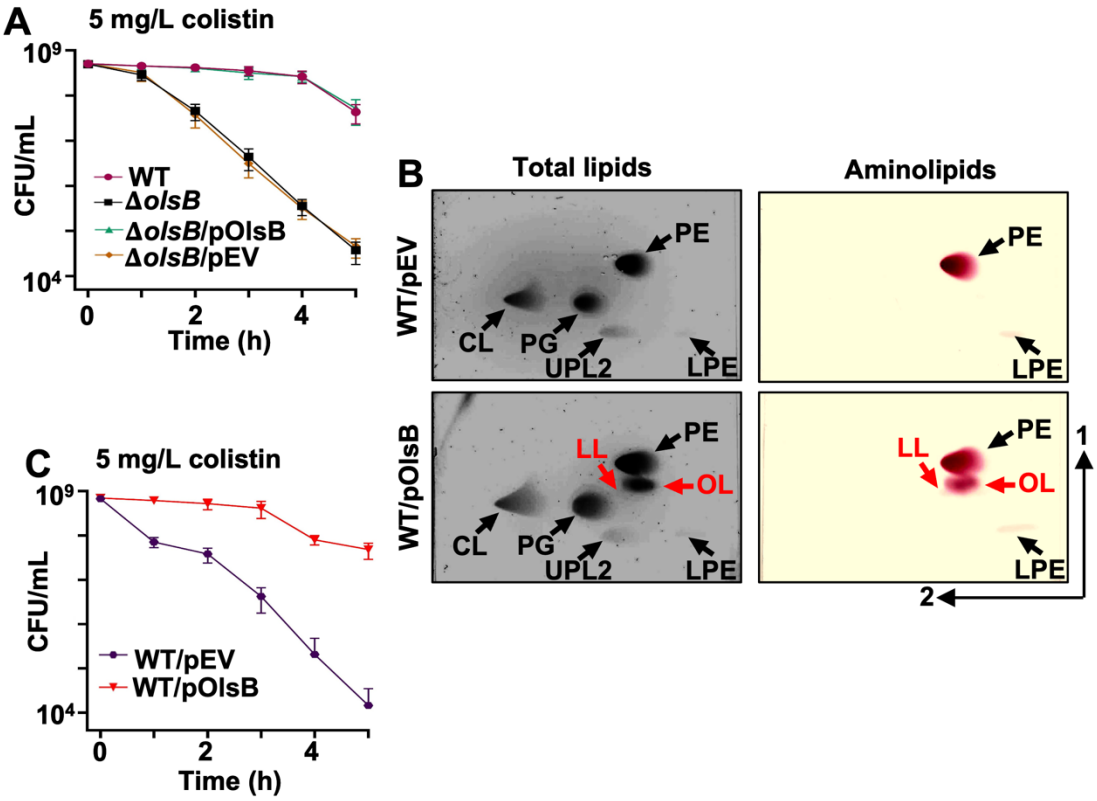

Figure 4: Aminolipids promote colistin tolerance in *A. baumannii*. A. Colistin-dependent killing in wild type and Δ*olsB* mutant strains. $n = 3$. Error bars indicate standard deviation. Wild type (WT) strains carrying pOlsB or empty vector were subjected to 5 mg/L colistin exposure over time. CFU/mL were calculated every 0.5 h. **B.** Total lipids were extracted using the Bligh and Dyer method and separated using 2D thin-layer chromatography. Lipids were stained with sulfuric acid (left). Aminolipids were stained using ninhydrin (right). Specific lipids are labelled: PE, phosphatidylethanolamine; PG, phosphatidylglycerol; CL, cardiolipin; LPE, lyso-phosphatidylethanolamine; LL, lysine lipid; OL, ornithine lipid; U3, unknown lipid 3. OL and LL are labelled in red. **C.** Colistin-dependent kill curves (left) and growth rate analysis (right) in wild type expressing empty vector (pEV) or pOlsB ($n = 3$). Error bars indicate standard deviation.

277 **Figure S5A**), suggesting the antibiotic could be more effective against *A. baumannii* when
278 aminolipid biosynthesis is inhibited. Overexpression of *olsB* in wild-type *A. baumannii* was
279 sufficient to produce aminolipids during cultivation in excess phosphate (**Figure 4B**).
280 Analysis demonstrated that *olsB* induction led to increased colistin tolerance (**Figure 4C and**
281 **Figure S5B**). Therefore, OlsB-dependent aminolipid biosynthesis in *A. baumannii* promotes
282 colistin tolerance, a last-line antibiotic for combating multidrug-resistant Gram-negative
283 bacteria.
284

285 **PhoR regulates aminolipid biosynthesis in *A. baumannii***

286 Previous work established that aminolipid production generally occurs in response to
287 phosphate limitation (6, 14, 15, 34, 35). Consequently, we expected to find a Pho box
288 upstream of the putative *olsB* gene. Using the *E. coli* pho box consensus sequence (36), a
289 putative Pho box was identified that precedes the *olsB* gene in diverse *Acinetobacter* isolates,

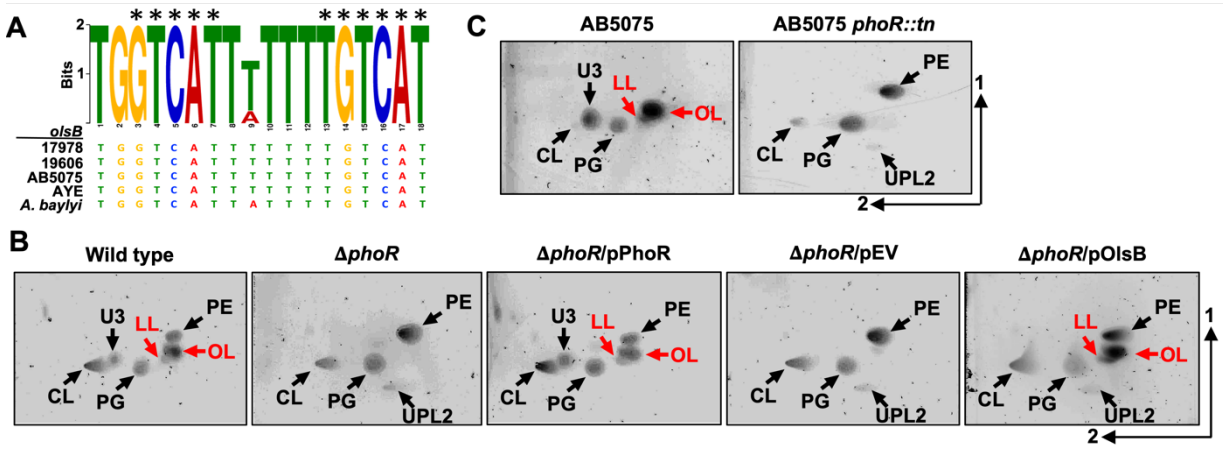

Figure 5: PhoR regulates *olsB* gene expression and aminolipid formation in *A. baumannii* strains. **A.** Predicted Pho box sequence alignments from *A. baumannii* strain 17978, 19606, AB5075, AYE, and *A. baylyi olsB* promoters. Black asterisks represent conserved nucleotides in the *E. coli* Pho box consensus (CT*GTCAT*NNNNC*TGTCAT*). **B.** 2D thin-layer chromatography lipid analysis from *A. baumannii* strain ATCC 17978 wild type and mutants grown in minimal media supplemented with 50 µM (limiting) phosphate. **C.** 2D thin-layer chromatography lipid analysis from *A. baumannii* strain AB5075 wild type and the *phoR* Tn*26* mutant in minimal media supplemented with 50 µM (limiting) phosphate. Lipids were stained with sulfuric acid. OL and LL aminolipids are labelled in red.

290 including ATCC 17978 (**Figure 5A**), but not preceding the *olsA* gene. These results are
291 consistent with our transcriptomics analysis, which also suggested *olsA* gene expression is
292 not responsive to phosphate concentrations.

293 Phosphate sensing and diverse responses are regulated by the two-component system,
294 PhoB/PhoR, in many bacteria (37). When phosphate levels decrease, the sensor kinase, PhoR,
295 becomes activated, leading to autophosphorylation. Subsequent phosphotransfer to the
296 cognate response regulator, PhoB results in a conformational change and DNA binding (38)
297 at target promoters to induce gene expression.

298 These findings imply that the PhoB/PhoR two-component system regulates OL and
299 LL biosynthesis in *A. baumannii* through *olsB* expression. To validate this hypothesis, we
300 generated Δ*phoR* (*A1S_3376*) in *A. baumannii* ATCC 17978 by fusing codon 65 to 410. Lipid
301 analysis after growth limiting phosphate, showed that the Δ*phoR* mutant accumulates
302 glycerophospholipids PE, PG, CL, and UPL2, while failing to synthesize OL, LL, and U3,
303 unlike the wild-type strain (**Figure 5B**). Complementation of the *phoR*-deficient mutant with
304 the PhoR allele restored OL and LL formation, while aminolipids were absent in the mutant
305 carrying the empty vector. Expression of *olsB* from a non-native locus in the Δ*phoR* mutant
306 restored OL and LL biosynthesis. Additionally, we examined the lipid patterns of the *phoR*
307 (ABUW_0105)-transposon mutant of *A. baumannii* AB5075 grown under phosphate
308 limitation (**Figure 5C**). Lipidomic analysis revealed that, unlike the wild-type strain, the
309 *phoR::tn* mutant predominantly accumulated phospholipids and was unable to produce OL
310 or LLs. Together, these findings suggest that *olsB* expression in *A. baumannii* is mediated by
311 the *phoR* regulatory gene.
312

313 **Other Gram-negative ESKAPE pathogens form aminolipids under conditions of**
314 **phosphate depletion**

315 In addition to *P. aeruginosa* (14), *A. baumannii* is the second Gram-negative ESKAPE
316 bacterium where the OL biosynthesis has been described using a OlsBA-dependent
317 mechanisms. Uniquely, *A. baumannii* also produces LL via the same pathway. These findings
318 prompted us to investigate if other Gram-negative ESKAPE pathogens, such as *Klebsiella* or
319 *Enterobacter*, are also capable of aminolipid biosynthesis under phosphate limitation. TLC
320 analysis of total lipids from *K. pneumoniae*, *E. cloacae* or *P. aeruginosa* after growth in
321 minimal medium supplemented with excess phosphates showed production of the canonical

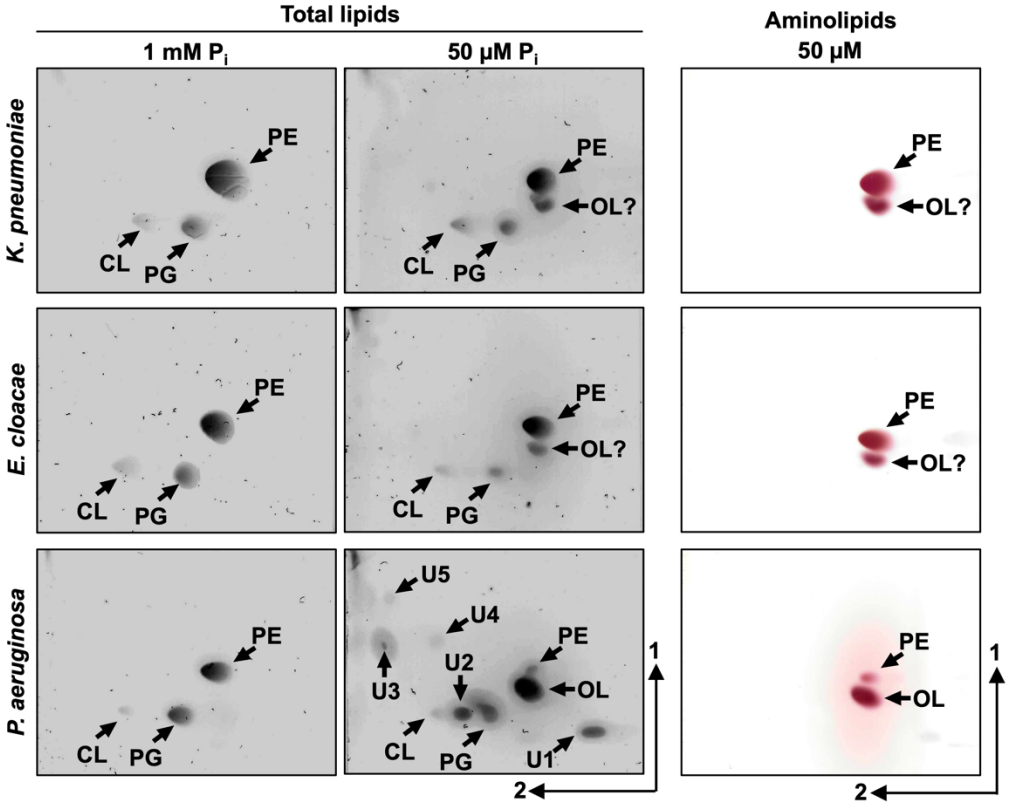

Figure 6: Aminolipid biosynthesis is conserved in Gram-negative ESKAPE pathogens. 2D thin-layer chromatography of lipids extracted from wild type *K. pneumoniae* strain KPNIH1, *E. cloacae* strain ATCC 13047, and *P. aeruginosa* strain PAO1 grown in excess (1 mM) or limiting (50 µM) phosphate conditions. Totals lipids were stained with sulfuric acid (left). Aminolipids were stained using ninhydrin (right). Specific lipids are labelled: PE, phosphatidylethanolamine; PG, phosphatidylglycerol; CL, cardiolipin; OL, ornithine lipid; U1, U2, U3, U4, and U5; unknown compounds 1, 2, 3, 4, and 5.

322 membrane phospholipids PE, PG, and CL (**Figure 6**). However, when cultivating *P.*
323 *aeruginosa* in phosphate limitation (50 μM), a significant decrease in relative phospholipid
324 levels was observed, and the synthesis of five unknown compounds and OL was induced. *K.*
325 *pneumoniae* and *E. cloacae* cultivated in low phosphate concentrations (50 μM), also showed
326 decreased levels of phospholipid production and accumulation of an unknown lipid. The
327 unknown lipid exhibited a migration pattern and ninhydrin staining on TLC like OL,
328 suggesting that aminolipid biosynthesis may be a conserved response to phosphate limiting
329 growth conditions that could promote tolerance to antibiotics in Gram-negative ESKAPE
330 pathogens.
331
332 **Discussion**
333 Bacteria have evolved various regulatory mechanisms to sense and adapt to
334 environmental stress. Here, we show that under phosphate-limiting conditions, *A. baumannii*
335 produces ornithine and lysine lipids through regulated expression of *olsB*. The aminolipids
336 alter the lipid bilayer composition to promote tolerance to colistin, an antimicrobial peptide
337 used to treat Gram-negative bacterial infections. Specifically, aminolipids could reduce the
338 electrostatic potential for cationic antimicrobial peptides such as colistin to target the cell,
339 emphasizing changes in bilayer charge as an adaptive mechanism for *A. baumannii* in
340 challenging environments. Broadly, cell membrane lipid modifications are vital for bacterial
341 survival upon exposure to antimicrobial cationic peptides. For example, *V. cholerae* modifies
342 lipid A with glycine or diglycine residues to resist cationic antimicrobial peptides (39).
343 Similar strategies are employed by various bacterial species, such as *P. aeruginosa*,
344 *Rhizobium tropici*, *Staphylococcus aureus*, *Mycobacterium tuberculosis*, and *Bacillus*

345 *subtilis*, which modify phospholipids like PG by adding amino acids like lysine or alanine,
346 thereby conferring polymyxins resistance (34, 35, 40–42).

347 Membrane lipid remodeling during growth under phosphate limitation is a conserved
348 strategy across bacteria, involving the substitution of phospholipids with phosphorus-free
349 lipids alternatives like aminolipids (43). While the synthesis of these lipids is not directly
350 induced by the presence of polymyxins, tolerance to polymyxins is an indirect consequence
351 of lipid membrane remodeling, leading to significant changes in membrane chemical
352 properties. The alteration could reduce the net negative charge of the membrane, thereby
353 decreasing CAMP susceptibility.

354 The *olsB* gene is required for OL biosynthesis, but unlike other OlsB-dependent
355 pathways, it also induces LL formation in *A. baumannii*, suggesting metabolic plasticity
356 within the species. Comparing our findings with observations in other bacteria, such as the
357 soil bacterium *Rhodobacter sphaeroides*, which not only produces OLs but also synthesizes
358 glutamine lipids (GLs) (44), further highlights the metabolic diversity in aminolipid
359 biosynthesis. Additionally, recent research has shown that marine bacteria *Ruegeria*
360 *pomeroyi* encode two *olsB* paralogs, one responsible for forming OLs and the other for GLs
361 (33). Although these bacteria inhabit vastly different environments, the similarities suggest
362 that the ability to use multiple substrates for aminolipid synthesis may be a common survival
363 strategy in variable environmental conditions.

364 The transcriptomic analysis uncovered insights into different expression patterns of
365 the *olsB* and *olsA* genes in response to phosphate limitation. Specifically, overexpression of
366 the *olsB* gene was observed during phosphate limited growth, indicating a regulatory
367 mechanism. However, *olsA* expression remained unchanged. The predicted Pho box in the
368 promoter region of *olsB* suggested that the PhoB/PhoR two-component system regulates *olsB*

369 under phosphate limitation conditions. Conversely, the absence of a similar motif in the
370 promoter region of *olsA* implies the influence of other regulatory factors on its expression,
371 independent of phosphate availability. Furthermore, *olsB* overexpression with non-native
372 promoter in *A. baumannii* during cultivation in excess phosphate resulted in aminolipid
373 formation, suggesting OlsA-dependent activity occurs after OlsB has formed a lyso-
374 aminolipid. The differential regulatory events may also suggest that OlsA utilizes other
375 substrates. For instance, in *Rhodobacter capsulatus*, OlsA functions as a bifunctional
376 enzyme, active in both OL and phosphatidic acid biosynthesis (45). Additionally, we
377 confirmed the role of the *phoR* gene as a key regulator in aminolipid biosynthesis in *A.*
378 *baumannii*, highlighting its fine-tuned regulation in response to environmental stressors such
379 as phosphate limitation. Interestingly, this regulatory mechanism shares similarities with
380 species like *Sinorhizobium meliloti* or *V. cholerae*, where PhoB/PhoR also regulates OLs
381 synthesis under phosphate limitation conditions (6, 15), underscoring the evolutionary
382 conservation of these adaptive mechanisms across different bacterial taxa.

383 Finally, the presence of *olsB* and *olsA* orthologues in *A. baumannii* raises questions
384 about the diversity of aminolipid biosynthesis pathways among pathogens. Interestingly,
385 bacteria such as *Klebsiella* and *Enterobacter* lack these orthologs, suggesting distinct
386 biosynthesis pathways compared to *A. baumannii*. This absence prompts further investigation
387 into alternative pathways or genes involved in aminolipid synthesis and their implications
388 for antibiotics resistance and environmental adaptation.

389

390 **Conclusion**

391 The study highlights the impact of phosphate limitation on lipid membrane
392 composition in *A. baumannii*, resulting in the synthesis of OLs and LLs through regulated

393 *olsB* gene expression. Aminolipids can promote tolerance to colistin, an important last-line
394 antimicrobial. These results also underscore the role for *phoR* gene in regulating aminolipid
395 synthesis in *A. baumannii* and show that other Gram-negative ESKAPE pathogens produce
396 aminolipids under phosphate-depleted conditions. Aminolipid biosynthesis is a common
397 adaptive response to phosphate limitation, which could promote pathogen survival both in
398 hospital environment and within the host.
399

400 **Materials and methods**

401 **Bacterial strains and growth.** All strains and plasmids used in this study are listed in Table
402 S4 in the supplemental material. *E. coli*, *Acinetobacter* strains, *K. pneumoniae*, *E. cloacae* or
403 *P. aeruginosa* were initially cultured from frozen stocks on Luria-Bertani (LB Miller) agar at
404 37ºC. Isolated colonies were used to inoculate LB Miller broth or minimal medium (Tris
405 minimal succinate [TMS]) (46); supplemented with different phosphate concentrations at
406 37ºC. The minimal medium included: Na-succinate 20 mM, NaCl 200 mg/mL, NH_4Cl 450
407 mg/mL, $CaCl_2$ 200 mg/mL, KCl 200 mg/mL, $MgCl_2$ 450 mg/mL, $FeCl_2$ 10 mg/L, and $MnCl_2$
408 10 mg/L, with 10 mM 4-(2-hydroxyethyl)-1-piperazineethanesulfonic acid (HEPES) buffer
409 used at pH 7.2. Na_2HPO_4 was then added to achieve a final concentration of 1 mM (excess)
410 or 50 µM (limiting). All components were dissolved in deionized water and sterilized by
411 filtration trough 0.22 µm pore-size filters and dissolved deionized H_2O. To generate growth
412 curves, overnight cultures of *A. baumannii* strains were diluted to an OD_{600} of ~0.05 in 5 mL
413 of medium, then incubated in glass test tubes at 37ºC for 24 hours. Growth curve data were
414 analyzed and plotted using GraphPad Prism software.
415

416 **Construction of mutant and complementation *A. baumannii* strains.** The primers utilized
417 in this study are listed in Table S5 in the supplementary material. Genetic mutants of *A.*
418 *baumannii* were generated following established protocols (47–50). Briefly, *A. baumannii*
419 carrying the pMMB67EH^{TetR} plasmid containing the REC$_{Ab}$ coding sequences was diluted
420 from an overnight culture into LB Miller broth containing 10µg/mL of tetracycline at an
421 OD_{600} of ~0.05 and incubated for 45 minutes. REC$_{Ab}$ expression was induced by adding 2
422 mM IPTG, and cells were cultured at 37ºC until they reached mid-log growth phase (OD_{600}
423 of ~0.4). After washing the cells three times in ice-cold 10% glycerol, 10^{10} cells were
424 electroporated in a 2-mm cuvette at 1.8 mV with 5 µg of a recombineering linear PCR
425 product. Subsequently, the cells were cultured for 4 hours in 4 mL of LB Miller broth with 2
426 mM IPTG and then plated on LB agar supplemented with 20 µg/mL of kanamycin. Mutations
427 were validated using PCR.

428 To cure isolated mutants of the pMMB67EH^{TetR}::REC$_{Ab}$ plasmid after mutant
429 isolation, strains were streaked for isolated colonies on LB Miller agar supplemented with 2
430 mM $NiCl_2$ to select cells that had lost the tetracycline cassette (48–51). Cured insertion
431 mutants were then electroporated with pMMB67EH^{TetR} carrying the FLP recombinase. Cells
432 were recovered for 1 hour in 5 mL of LB Miller broth and plated on LB agar containing
433 10µg/mL of tetracycline and 2 mM IPTG to induce expression of the FLP recombinase.
434 Excision of the kanamycin cassette was confirmed by PCR.

435 To complement the *A. baumannii* ATCC 17978 mutants, the coding sequence from
436 *A1S_0889* (*olsB*) was cloned into the KpnI/SalI sites, while the coding sequence from
437 *A1S_3376* (*phoR*) was cloned into the KpnI/BamHI sites in pMMB67EH^{KanR}. Plasmids were
438 expressed in the respective mutants, and all strains were grown in 30 µg/mL of kanamycin
439 and 1 mM IPTG for expression.

440

441 **Analysis of total lipids and aminolipids.** Overnight cultures were used to inoculate 10 mL
442 minimal medium 1 mM phosphate, or 20 mL minimal medium 50 μM phosphate to achieve
443 an OD_{600} of ~0.05, and then incubated for 24 hours at 37 ºC. After the incubation period, cells
444 were collected by centrifugation. Lipids were extracted using the Bligh and Dyer (1959)
445 method (52). The chloroform phase was separated into the individual components on high-
446 performance TLC silica gel plates. For one-dimensional TLC analysis, the plates were
447 developed with chloroform-methanol-water (130:50:8 v/v) mixture. For two-dimensional
448 TLC analysis, a chloroform-methanol-water (140:60:10 v/v) mixture was used in the first
449 dimension and chloroform-methanol-acetic acid (130:50:20 v/v) mixture was used in the
450 second dimension. Lipids on TLC were visualized by treating the plates with 10% sulfuric
451 acid in ethanol at 150ºC (total lipids) or 0.2% ninhydrin in acetone at 100ºC (aminolipids).

452

453 **Analysis of ^{32}P-labeled phospholipids.** Overnight cultures were diluted to an OD_{600} of ~0.05
454 in 10 mL LB Miller broth supplemented with 5 μCi/mL ^{32}P ortho-phosphoric acid
455 (PerkinElmer) and grown until reaching an OD_{600} of ~0.6. After harvesting the cells, lipid
456 extraction was performed using Bligh and Dyer method (52), followed by analysis using TLC
457 as previously described. Subsequently, the TLC plates were dried, exposed to a
458 phosphorimaging screen, and scanned using an Amersham Typhoon laser scanner.

459

460 **Liquid chromatography:** Aminolipids were separated by reversed phase liquid
461 chromatography (LC) using an Acquity UPLC CSH C18 column (pore size 130 Å, 1.7 μm
462 particle size, 2.1 mm × 100 mm, Waters) integrated with a Dionex Ultimate 3000 UHPLC
463 system (Thermo Fisher Scientific). Mobile phases A and B were comprised of methanol:

464 water: acetonitrile (3:4:3) and isopropanol: water: acetonitrile (90:2.5:7.5), respectively, each
465 containing 10 mM ammonium formate. Dried lipid content from TLC separations and Bligh
466 and Dyer extractions were resuspended in 50:50 mobile phase A: B at a concentration of
467 ~100 ng/uL. A 9 uL injection volume was used, and the column compartment was maintained
468 at a temperature of 50 °C. Aminolipids were separated at a flow rate of 0.275 mL/min with
469 the following gradient: hold at 10% B (0-1 min), 10-45% B (1-5 min), 45-70% B (5-23 min),
470 70-95% B (23-24 min), hold at 95% B (24-29 min), 95-10% B (29-29.5), and hold at 10% B
471 (29.5-35 min).
472
473 **Untargeted LC-MS with HCD and Targeted LC-MS with UVPD Experiments:** An
474 untargeted negative-ionization mode LC-MS-HCD method was utilized to screen lipid
475 extracts on a Thermo Scientific Orbitrap Fusion Lumos Tribrid mass spectrometer via heated
476 electrospray ionization. Various source parameters included a spray voltage of -3800 V,
477 sheath gas setting of 5, aux gas setting of 10, and ion transfer tube temperature of 300 °C.
478 MS1 data was collected at a resolution of 30,000 at *m/z* 200 in the orbitrap analyzer with a
479 scan range of *m/z* 500-1000, RF lens of 80%, and an AGC target of 5E5. A data dependent
480 acquisition method was used in which the five most abundant ions above an intensity
481 threshold of 5E4 were selected for MS/MS analysis with HCD. Species were isolated using
482 a 1 *m/z* window and subjected to an HCD collision energy of 22%. MS2 spectra were
483 acquired at a resolution of 30,000 at *m/z* 200 in the orbitrap, q-value of 0.1, AGC target of
484 1E5, maximum injection time of 250 ms, and 2 microscans/scan. Data was manually
485 interpreted using Thermo Xcaliber Qual Browser.
486 A targeted positive-ionization mode LC-MS/MS method was performed on a Thermo
487 Scientific Orbitrap Eclipse Tribrid mass spectrometer equipped with an ArF excimer laser

488 (Coherent, Inc.) for 193 nm UVPD. The heated electrospray ionization source was operated
489 at +3800 V, and the source parameters described above were implemented. MS/MS scans
490 with UVPD were acquired in a data dependent manner, with 5 scans collected between each
491 MS1 master scan and an intensity threshold set at 5E4. A targeted mass filter was employed
492 that included the *m/z* values and start/end retention times for unsaturated aminolipids
493 identified from the negative-ionization mode LC-MS with HCD run (with a 15-ppm error
494 tolerance). Aminolipids were isolated with a 1 *m/z* window and activated with 4 laser pulses
495 at 2 mJ/pulse for double bond localization. MS^2 spectra were acquired at a resolution of
496 30,000 at *m/z* 200 in the orbitrap analyzer, q-value of 0.1, AGC target of 5E5, maximum
497 injection time of 500 ms, and 5 microscans/scan.
498
499 **RNA sequencing.** Transcriptome sequencing analysis was performed as described
500 previously, with modification (50). Briefly, total RNA was extracted from *A. baumannii*
501 ATCC 17978 cultures grown in minimal medium supplemented with either excess (1 mM)
502 or limiting (50 μM) phosphate at OD_{600} of ~0.5 in triplicate, utilizing the Direct-Zol RNA
503 miniprep kit (Zymo Research). Genomic DNA contamination was eliminated using the Turbo
504 DNA-free DNA removal kit (Invitrogen). DNAase-treated RNA samples were then
505 forwarded to SeqCenter for sequencing on the Illumina NextSeq 550 sequencing.
506 Subsequently, the CLC Genomic Workbench software (Qiagen) was employed to map the
507 obtained sequencing data to the *A. baumannii* ATCC 17978 genome annotations and
508 determine the read per kilobase per million (RPKM) expression values and determine the
509 weighted-proportions fold changes in expression values between excess or limitation
510 phosphate conditions. Data were analyzed and plotted using GraphPad Prism software. Data
511 Accession #: GSE276010.

512

513 **Microscopy and image analysis.** Cells were grown as stated above and fixed with
514 paraformaldehyde (PFA) and mounted on 1.5% agarose in 1X phosphate-buffered saline
515 (PBS). Imaging was performed using a Nikon Eclipse Ti-2 wide-field epifluorescence
516 microscope equipped with a Photometrics Prime 95B camera and a Plan Apo 100x, 1.45
517 numerical aperture objective lens. Images were captured using NIS Elements software.
518 Image analysis was conducted using the microbeJ plugin of ImageJ software.

519

520 **LOS staining and analysis.** All cultures were grown in test tubes containing 5 mL of
521 minimal medium with either excess (1 mM) or limiting (50 μM) phosphate at 37°C in a
522 shaker overnight. For the complementation strains, 30 μg/mL kanamycin and 1 mM IPTG
523 were added. The OD_{600} of the overnight cultures was measured and normalized to OD_{600} of
524 ~1. The cells were then centrifuged at 15,000 rpm for 5 minutes. Each pellet was resuspended
525 in 100 μl of 1X Sample Buffer (4X LDS Sample Buffer, 4% β-mercaptoethanol, and water)
526 and boiled in water for 10 minutes. After cooling, proteinase K was added to each sample
527 and mixed. The samples were then incubated in a 55°C water bath overnight. The following
528 day, the samples were boiled in water for 5 minutes and SDS-PAGE was performed. The gel
529 was then fixed and treated according to the protocol in the Pro-Q Emerald 300
530 Lipopolysaccharide Gel Stain Kit by Thermo Fisher Scientific (P20495).

531

532 **Colistin susceptibility assays.** Overnight cultures were diluted to OD_{600} ~0.150 in minimal
533 medium supplemented with either excess (1 mM) or limiting (50 μM) phosphate containing
534 5 mg/L colistin. Each culture, comprising 15 mL, was incubated in 125 mL Erlenmeyer flasks

535 at 37ºC with agitation at 250 rpm. Survivors were analyzed at specific time points by serial
536 dilution plating on LB agar.
537
538 **Acknowledgments**
539 The work was supported by funding from the National Institutes of Health (grants
540 R35GM143053 and R01AI168159 to J.M.B and R35GM139658 to J.S.B), and the Robert A.
541 Welch Foundation (F-1155 to J.S.B.).
542
543
544 **References**
545 1. Raetz CRH, Whitfield C. 2002. Lipopolysaccharide endotoxins. *Annu Rev Biochem*
546 71:635–700.

547 2. Sohlenkamp C, Geiger O. 2016. Bacterial membrane lipids: diversity in structures and
548 pathways. *FEMS Microbiol Rev* 40:133–159.

549 3. Geiger O, González-Silva N, López-Lara IM, Sohlenkamp C. 2010. Amino acid-
550 containing membrane lipids in bacteria. *Prog Lipid Res* 49:46–60.

551 4. Moore EK, Hopmans EC, Rijpstra WIC, Villanueva L, Damsté JSS. 2016. Elucidation
552 and identification of amino acid containing membrane lipids using liquid
553 chromatography/high-resolution mass spectrometry. *Rapid Commun Mass Spectrom*
554 RCM 30:739–750.

555 5. Vences-Guzmán MÁ, Geiger O, Sohlenkamp C. 2012. Ornithine lipids and their
556 structural modifications: from A to E and beyond. *FEMS Microbiol Lett* 335:1–10.

557 6. Geiger O, Röhrs V, Weissenmayer B, Finan TM, Thomas-Oates JE. 1999. The regulator
558 gene *phoB* mediates phosphate stress-controlled synthesis of the membrane lipid
559 diacylglyceryl-N,N,N-trimethylhomoserine in *Rhizobium (Sinorhizobium) meliloti.*
560 *Mol Microbiol* 32:63–73.

561 7. Dees C, Shively JM. 1982. Localization of quantitation of the ornithine lipid of
562 *Thiobacillus thiooxidans*. *J Bacteriol* 149:798–799.

563 8. Palacios-Chaves L, Conde-Álvarez R, Gil-Ramírez Y, Zúñiga-Ripa A, Barquero-Calvo
564 E, Chacón-Díaz C, Chaves-Olarte E, Arce-Gorvel V, Gorvel J-P, Moreno E, de Miguel
565 M-J, Grilló M-J, Moriyón I, Iriarte M. 2011. *Brucella abortus* ornithine lipids are
566 dispensable outer membrane components devoid of a marked pathogen-associated
567 molecular pattern. *PloS One* 6:e16030.

568 9. Vences-Guzmán MÁ, Guan Z, Ormeño-Orrillo E, González-Silva N, López-Lara IM,
569 Martínez-Romero E, Geiger O, Sohlenkamp C. 2011. Hydroxylated ornithine lipids
570 increase stress tolerance in *Rhizobium tropici* CIAT899. *Mol Microbiol* 79:1496–1514.

571 10. Stirrup R, Mausz MA, Silvano E, Murphy A, Guillonneau R, Quareshy M, Rihtman B,
572 Ferretjans MA, He R, Todd JD, Chen F, Scanlan DJ, Chen Y. 2023. Aminolipids elicit
573 functional trade-offs between competitiveness and bacteriophage attachment in
574 *Ruegeria pomeroyi. ISME J* 17:315–325.

575 11. Weissenmayer B, Gao J-L, López-Lara IM, Geiger O. 2002. Identification of a gene
576 required for the biosynthesis of ornithine-derived lipids. *Mol Microbiol* 45:721–733.

577 12. Gao J-L, Weissenmayer B, Taylor AM, Thomas-Oates J, López-Lara IM, Geiger O.
578 2004. Identification of a gene required for the formation of lyso-ornithine lipid, an
579 intermediate in the biosynthesis of ornithine-containing lipids. *Mol Microbiol* 53:1757–
580 1770.

581 13. Vences-Guzmán MÁ, Guan Z, Escobedo-Hinojosa WI, Bermúdez-Barrientos JR,
582 Geiger O, Sohlenkamp C. 2015. Discovery of a bifunctional acyltransferase responsible
583 for ornithine lipid synthesis in *Serratia proteamaculans. Environ Microbiol* 17:1487–
584 1496.

585 14. Lewenza S, Falsafi R, Bains M, Rohs P, Stupak J, Sprott GD, Hancock REW. 2011. The
586 *olsA* gene mediates the synthesis of an ornithine lipid in *Pseudomonas aeruginosa*
587 during growth under phosphate-limiting conditions, but is not involved in antimicrobial
588 peptide susceptibility. *FEMS Microbiol Lett* 320:95–102.

589 15. Barbosa LC, Goulart CL, Avellar MM, Bisch PM, von Kruger WMA. 2018.
590 Accumulation of ornithine lipids in *Vibrio cholerae* under phosphate deprivation is
591 dependent on *VC0489* (OlsF) and PhoBR system. *Microbiol Read Engl* 164:395–399.

592 16. Harding CM, Hennon SW, Feldman MF. 2018. Uncovering the mechanisms of
593 *Acinetobacter baumannii* virulence. *Nat Rev Microbiol* 16:91–102.

594 17. Rojas-Jiménez K, Sohlenkamp C, Geiger O, Martínez-Romero E, Werner D, Vinuesa P.
595 2005. A ClC chloride channel homolog and ornithine-containing membrane lipids of
596 *Rhizobium tropici* CIAT899 are involved in symbiotic efficiency and acid tolerance.
597 *Mol Plant-Microbe Interact* MPMI 18:1175–1185.

598 18. González-Silva N, López-Lara IM, Reyes-Lamothe R, Taylor AM, Sumpton D,
599 Thomas-Oates J, Geiger O. 2011. The dioxygenase-encoding *olsD* gene from
600 *Burkholderia cenocepacia* causes the hydroxylation of the amide-linked fatty acyl
601 moiety of ornithine-containing membrane lipids. *Biochemistry* 50:6396–6408.

602 19. Boll JM, Tucker AT, Klein DR, Beltran AM, Brodbelt JS, Davies BW, Trent MS. 2015.
603 Reinforcing Lipid A Acylation on the Cell Surface of *Acinetobacter baumannii*
604 Promotes Cationic Antimicrobial Peptide Resistance and Desiccation Survival. *mBio*
605 6:e00478-00415.

606 20. Boll JM, Crofts AA, Peters K, Cattoir V, Vollmer W, Davies BW, Trent MS. 2016. A
607 penicillin-binding protein inhibits selection of colistin-resistant, lipooligosaccharide-
608 deficient *Acinetobacter baumannii*. *Proc Natl Acad Sci U S A* 113:E6228–E6237.

609 21. Kang KN, Klein DR, Kazi MI, Guérin F, Cattoir V, Brodbelt JS, Boll JM. 2019. Colistin
610 heteroresistance in *Enterobacter cloacae* is regulated by PhoPQ-dependent 4-amino-4-
611 deoxy-l-arabinose addition to lipid A. *Mol Microbiol* 111:1604–1616.

612 22. Murtha AN, Kazi MI, Schargel RD, Cross T, Fihn C, Cattoir V, Carlson EE, Boll JM,
613 Dörr T. 2022. High-level carbapenem tolerance requires antibiotic-induced outer
614 membrane modifications. *PLoS Pathog* 18:e1010307.

615 23. Ernst CM, Peschel A. 2011. Broad-spectrum antimicrobial peptide resistance by MprF-
616 mediated aminoacylation and flipping of phospholipids. *Mol Microbiol* 80:290–299.

617 24. Needham BD, Trent MS. 2013. Fortifying the barrier: the impact of lipid A remodelling
618 on bacterial pathogenesis. *Nat Rev Microbiol* 11:467–481.

619 25. Henderson JC, Zimmerman SM, Crofts AA, Boll JM, Kuhns LG, Herrera CM, Trent
620 MS. 2016. The Power of Asymmetry: Architecture and Assembly of the Gram-Negative
621 Outer Membrane Lipid Bilayer. *Annu Rev Microbiol* 70:255–278.

622 26. de Rudder KE, Thomas-Oates JE, Geiger O. 1997. Rhizobium meliloti mutants
623 deficient in phospholipid N-methyltransferase still contain phosphatidylcholine. *J*
624 *Bacteriol* 179:6921–6928.

625 27. Raetz CR, Dowhan W. 1990. Biosynthesis and function of phospholipids in *Escherichia*
626 *coli. J Biol Chem* 265:1235–1238.

627 28. Lopalco P, Stahl J, Annese C, Averhoff B, Corcelli A. 2017. Identification of unique
628 cardiolipin and monolysocardiolipin species in *Acinetobacter baumannii. Sci Rep*
629 7:2972.

630 29. Stankeviciute G, Guan Z, Goldfine H, Klein EA. 2019. *Caulobacter crescentus* Adapts
631 to Phosphate Starvation by Synthesizing Anionic Glycoglycerolipids and a Novel
632 Glycosphingolipid. *mBio* 10:e00107-19.

633 30. Escobedo-Hinojosa WI, Vences-Guzmán MÁ, Schubotz F, Sandoval-Calderón M,
634 Summons RE, López-Lara IM, Geiger O, Sohlenkamp C. 2015. OlsG (Sinac_1600) Is
635 an Ornithine Lipid N-Methyltransferase from the Planctomycete *Singulisphaera*
636 *acidiphila. J Biol Chem* 290:15102–15111.

637 31. Kim S-K, Park S-J, Li X-H, Choi Y-S, Im D-S, Lee J-H. 2018. Bacterial ornithine lipid,
638 a surrogate membrane lipid under phosphate-limiting conditions, plays important roles
639 in bacterial persistence and interaction with host. *Environ Microbiol* 20:3992–4008.

640 32. Gallagher LA, Ramage E, Weiss EJ, Radey M, Hayden HS, Held KG, Huse HK,
641 Zurawski DV, Brittnacher MJ, Manoil C. 2015. Resources for Genetic and Genomic
642 Analysis of Emerging Pathogen *Acinetobacter baumannii. J Bacteriol* 197:2027–2035.

643 33. Smith AF, Rihtman B, Stirrup R, Silvano E, Mausz MA, Scanlan DJ, Chen Y. 2019.
644 Elucidation of glutamine lipid biosynthesis in marine bacteria reveals its importance
645 under phosphorus deplete growth in *Rhodobacteraceae. ISME J* 13:39–49.

646 34. Hebecker S, Arendt W, Heinemann IU, Tiefenau JHJ, Nimtz M, Rohde M, Söll D,
647 Moser J. 2011. Alanyl-phosphatidylglycerol synthase: mechanism of substrate
648 recognition during tRNA-dependent lipid modification in *Pseudomonas aeruginosa*.
649 *Mol Microbiol* 80:935–950.

650 35. Arendt W, Hebecker S, Jäger S, Nimtz M, Moser J. 2012. Resistance phenotypes
651 mediated by aminoacyl-phosphatidylglycerol synthases. *J Bacteriol* 194:1401–1416.

652 36. Baek JH, Lee SY. 2006. Novel gene members in the Pho regulon of *Escherichia coli*.
653 *FEMS Microbiol Lett* 264:104–109.

654 37. Hsieh Y-J, Wanner BL. 2010. Global regulation by the seven-component Pi signaling
655 system. *Curr Opin Microbiol* 13:198–203.

656 38. Gardner SG, McCleary WR. 2019. Control of the *phoBR* Regulon in *Escherichia coli.*
657 *EcoSal Plus 8*.

658 39. Hankins JV, Madsen JA, Giles DK, Brodbelt JS, Trent MS. 2012. Amino acid addition
659 to Vibrio cholerae LPS establishes a link between surface remodeling in gram-positive
660 and gram-negative bacteria. *Proc Natl Acad Sci U S A* 109:8722–8727.

661 40. Sohlenkamp C, Galindo-Lagunas KA, Guan Z, Vinuesa P, Robinson S, Thomas-Oates
662 J, Raetz CRH, Geiger O. 2007. The lipid lysyl-phosphatidylglycerol is present in
663 membranes of *Rhizobium tropici* CIAT899 and confers increased resistance to
664 polymyxin B under acidic growth conditions. *Mol Plant-Microbe Interact MPMI*
665 20:1421–1430.

666 41. Klein S, Lorenzo C, Hoffmann S, Walther JM, Storbeck S, Piekarski T, Tindall BJ, Wray
667 V, Nimtz M, Moser J. 2009. Adaptation of *Pseudomonas aeruginosa* to various
668 conditions includes tRNA-dependent formation of alanyl-phosphatidylglycerol. *Mol*
669 *Microbiol* 71:551–565.

670 42. Ernst CM, Staubitz P, Mishra NN, Yang S-J, Hornig G, Kalbacher H, Bayer AS, Kraus
671 D, Peschel A. 2009. The bacterial defensin resistance protein MprF consists of separable
672 domains for lipid lysinylation and antimicrobial peptide repulsion. *PLoS Pathog*
673 5:e1000660.

674 43. Geiger O, Padilla-Gómez J, López-Lara IM. 2019. Bacterial Sphingolipids and
675 Sulfonolipids, p. 123–137. *In* Geiger, O (ed.), Biogenesis of Fatty Acids, Lipids and
676 Membranes. Springer International Publishing, Cham.

677 44. Zhang X, Ferguson-Miller SM, Reid GE. 2009. Characterization of ornithine and
678 glutamine lipids extracted from cell membranes of *Rhodobacter sphaeroide*s. *J Am Soc*
679 *Mass Spectrom* 20:198–212.

680 45. Aygun-Sunar S, Bilaloglu R, Goldfine H, Daldal F. 2007. *Rhodobacter capsulatus* OlsA
681 is a bifunctional enzyme active in both ornithine lipid and phosphatidic acid
682 biosynthesis. *J Bacteriol* 189:8564–8574.

683 46. Jones RA, Shropshire H, Zhao C, Murphy A, Lidbury I, Wei T, Scanlan DJ, Chen Y.
684 2021. Phosphorus stress induces the synthesis of novel glycolipids in *Pseudomonas*
685 *aeruginosa* that confer protection against a last-resort antibiotic. *ISME J* 15:3303–3314.

686 47. Tucker AT, Nowicki EM, Boll JM, Knauf GA, Burdis NC, Trent MS, Davies BW. 2014.
687 Defining gene-phenotype relationships in *Acinetobacter baumannii* through one-step
688 chromosomal gene inactivation. *mBio* 5:e01313-01314.

689 48. Kang KN, Kazi MI, Biboy J, Gray J, Bovermann H, Ausman J, Boutte CC, Vollmer W,
690 Boll JM. 2021. Septal Class A Penicillin-Binding Protein Activity and ld-
691 Transpeptidases Mediate Selection of Colistin-Resistant Lipooligosaccharide-Deficient
692 *Acinetobacter baumannii. mBio* 12:e02185-20.

693 49. Kang KN, Boll JM. 2022. PBP1A Directly Interacts with the Divisome Complex to
694 Promote Septal Peptidoglycan Synthesis in *Acinetobacter baumannii. J Bacteriol*
695 204:e0023922.

696 50. Islam N, Kazi MI, Kang KN, Biboy J, Gray J, Ahmed F, Schargel RD, Boutte CC, Dörr
697 T, Vollmer W, Boll JM. 2022. Peptidoglycan Recycling Promotes Outer Membrane
698 Integrity and Carbapenem Tolerance in *Acinetobacter baumannii. mBio* 13:e0100122.

699 51. Podolsky T, Fong ST, Lee BT. 1996. Direct selection of tetracycline-sensitive
700 *Escherichia coli* cells using nickel salts. *Plasmid* 36:112–115.

52. Bligh EG, Dyer WJ. 1959. A rapid method of total lipid extraction and purification. *J Biochem Physiol* 37:911–917.

Figures

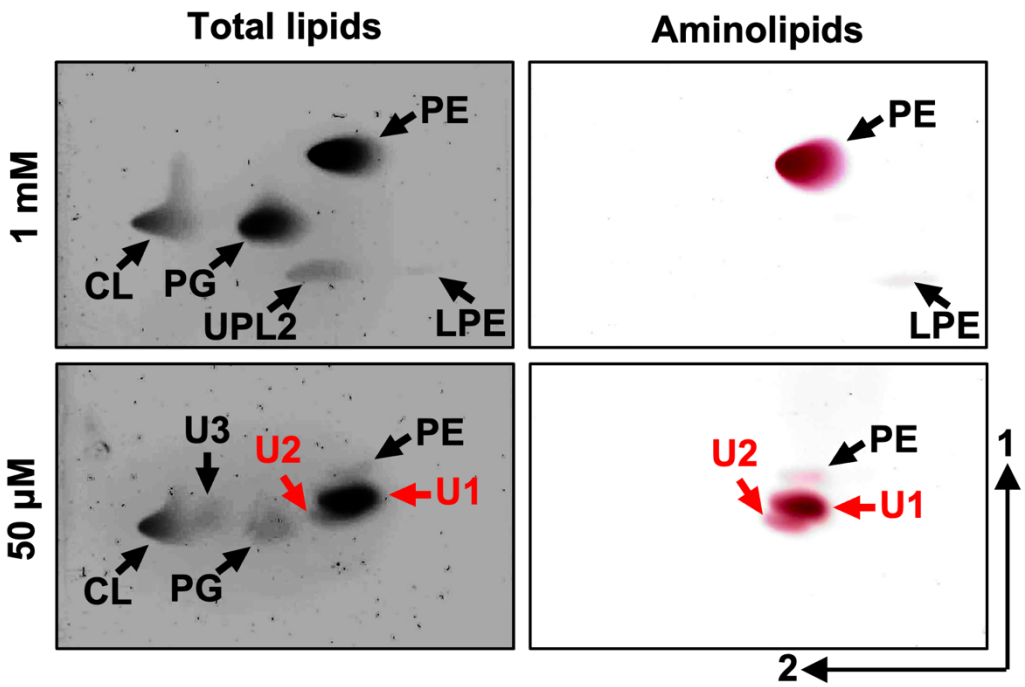

Figure 1: Lipid composition of *A. baumannii* strain ATCC 17978 in excess and limiting phosphate concentrations. Strains were grown in minimal with excess (1 mM) or limiting (50 µM) phosphate. Cells were collected, lipids were extracted using the Bligh and Dyer method and separated using 2-dimensional thin-layer chromatography. Total lipids were stained with sulfuric acid (left). Aminolipids were stained using ninhydrin (right). Specific lipids are labelled: PE, phosphatidylethanolamine; PG, phosphatidylglycerol; CL, cardiolipin; LPE, lyso-PE; U1, unknown lipid 1; U2, unknown lipid 2; U3, unknown lipid 3; UPL2, unknown phospholipid 2. Red letters denote aminolipids that provide the focus of the study.

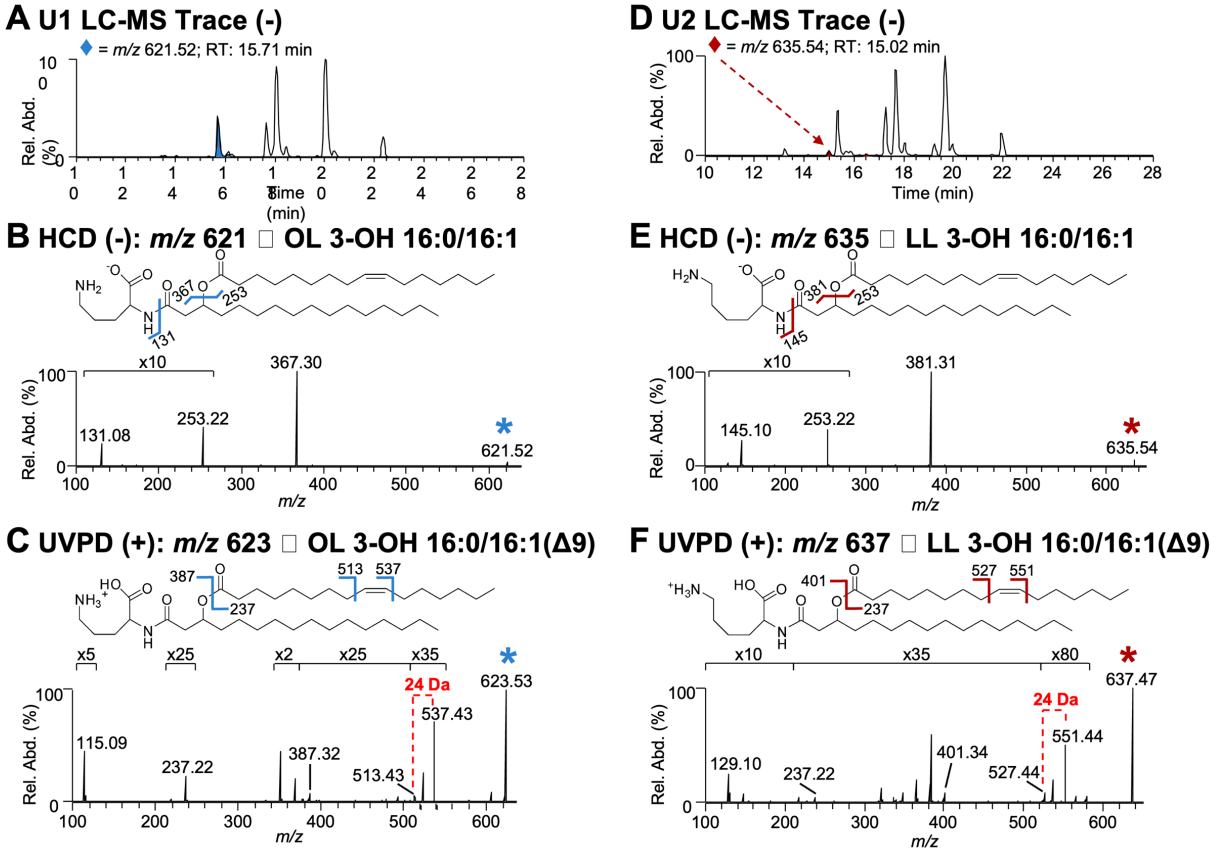

Figure 2: Structural analysis of the lipids produced during phosphate limitation. A. LC-MS trace of U1 lipid extract in negative ionization mode. **B.** HCD (NCE 22) mass spectrum of *m/z* 621.52 ($[M-H]^-$), an ornithine lipid found in U1 extract**. C.** UVPD (4 pulses at 2 mJ/pulse) mass spectrum of *m/z* 623.53 ($[M+H]^+$). **D.** LC-MS trace of U2 lipid extract in negative ionization mode. **E.** HCD (NCE 22) mass spectrum of *m/z* 635.54 ($[M-H]^-$), a lysine lipid found in U2 extract. **F.** UVPD (4 pulses at 2 mJ/pulse) mass spectrum of *m/z* 637.47 ($[M+H]^+$). The selected precursor ions are labeled with asterisks in B,C,E, and F.

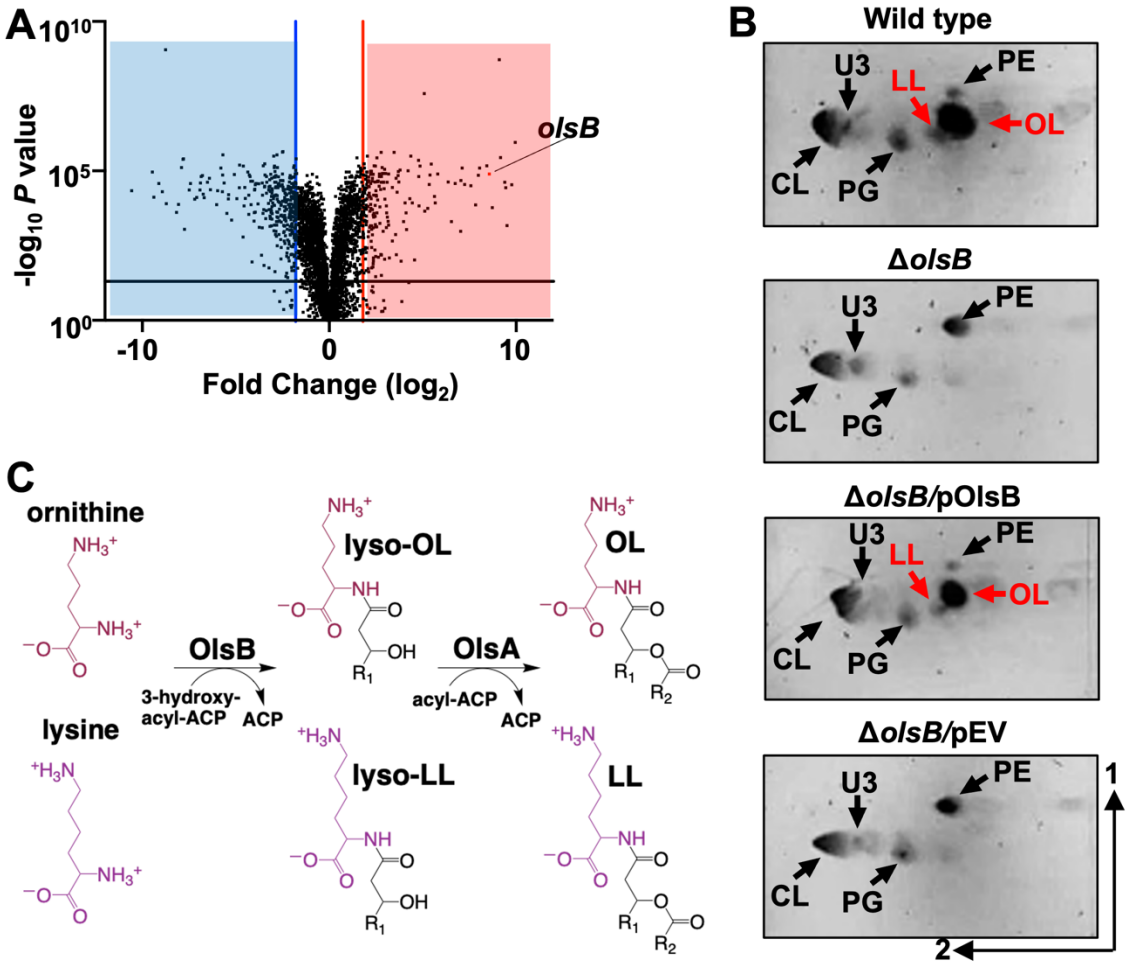

Figure 3: The *olsB* gene is required for ornithine and lysine lipid formation in phosphate limited growth conditions. A. Volcano plot of differentially regulated genes in excess and limiting phosphate. Red/blue lines indicate 3-fold cutoffs. The Black line on the *x*-axis indicates $P < 0.05$. A red dot representing the *olsB* expression profile is shown. **B.** 2D thin-layer chromatography stained with sulfuric acid showing wild type and Δ*olsB* strains grown in phosphate limiting (50 µM) conditions. Specific lipids are labelled: PE, phosphatidylethanolamine; PG, phosphatidylglycerol; CL, cardiolipin; OL, ornithine lipid; LL, lysine lipid; U3, unknown lipid 3. OL and LL aminolipids are labelled in red. **C.** Proposed ornithine lipid (OL) and lysine lipid (LL) biosynthesis pathways in *A. baumannii*.

732

733

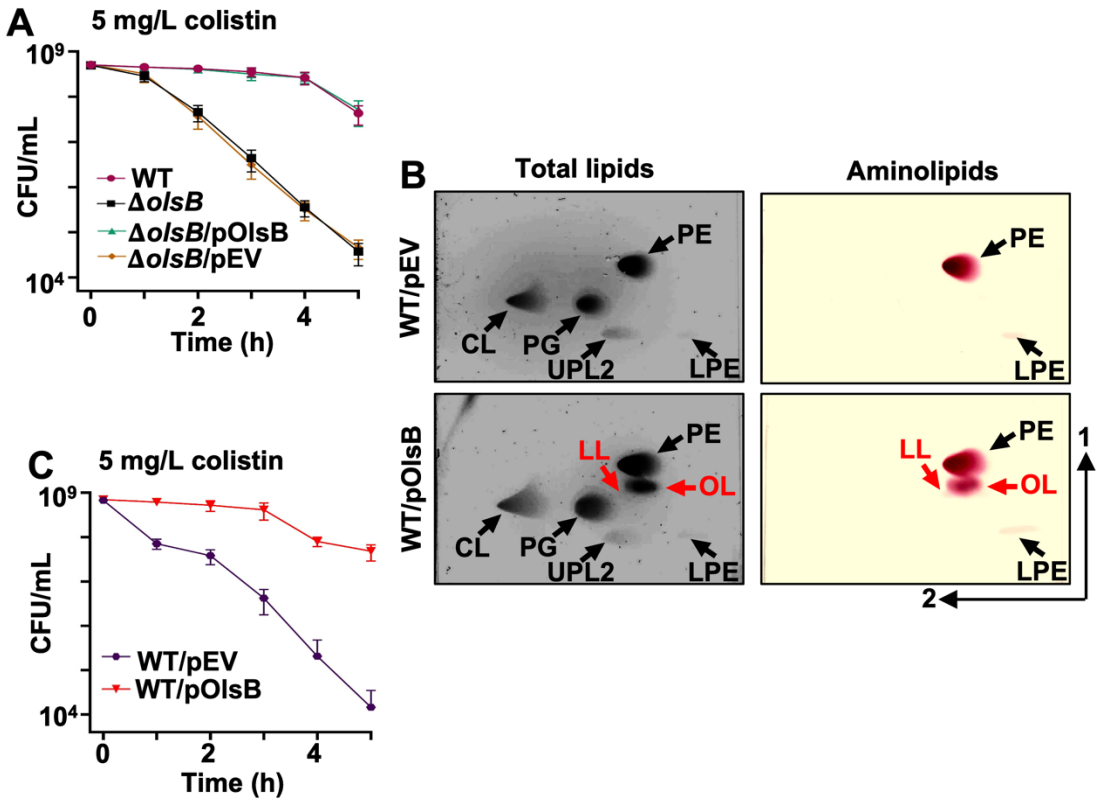

734 735 736 737 738 739 740 741 742 743 744

Figure 4: Aminolipids promote colistin tolerance in *A. baumannii*. A. Colistin-dependent killing in wild type and Δ*olsB* mutant strains. *n* = 3. Error bars indicate standard deviation. Wild type (WT) strains carrying pOlsB or empty vector were subjected to 5 mg/L colistin exposure over time. CFU/mL were calculated every 0.5 h. **B.** Total lipids were extracted using the Bligh and Dyer method and separated using 2D thin-layer chromatography. Lipids were stained with sulfuric acid (left). Aminolipids were stained using ninhydrin (right). Specific lipids are labelled: PE, phosphatidylethanolamine; PG, phosphatidylglycerol; CL, cardiolipin; LPE, lyso-phosphatidylethanolamine; LL, lysine lipid; OL, ornithine lipid; U3, unknown lipid 3. OL and LL are labelled in red. **C.** Colistin-dependent kill curves (left) and growth rate analysis (right) in wild type expressing empty vector (pEV) or pOlsB (*n* = 3). Error bars indicate standard deviation.

745 746 747 748

749

750

751

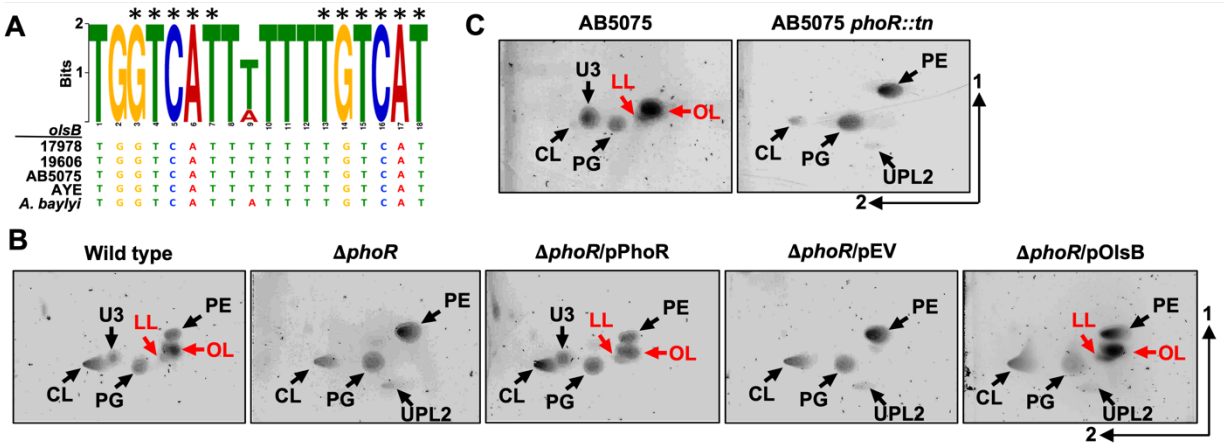

Figure 5: PhoR regulates *olsB* gene expression and aminolipid formation in *A. baumannii* strains. **A.** Predicted Pho box sequence alignments from *A. baumannii* strain 17978, 19606, AB5075, AYE, and *A. baylyi olsB* promoters. Black asterisks represent conserved nucleotides in the *E. coli* Pho box consensus (CT*GTCAT*NNNNNC*TGTCAT*). **B.** 2D thin-layer chromatography lipid analysis from *A. baumannii* strain ATCC 17978 wild type and mutants grown in minimal media supplemented with 50 µM (limiting) phosphate. **C.** 2D thin-layer chromatography lipid analysis from *A. baumannii* strain AB5075 wild type and the *phoR* Tn*26* mutant in minimal media supplemented with 50 µM (limiting) phosphate. Lipids were stained with sulfuric acid. OL and LL aminolipids are labelled in red.

752

753

754

755

756

757

758

759

760

761

762

763

764

765

766

767

768

769

770

771

772

773

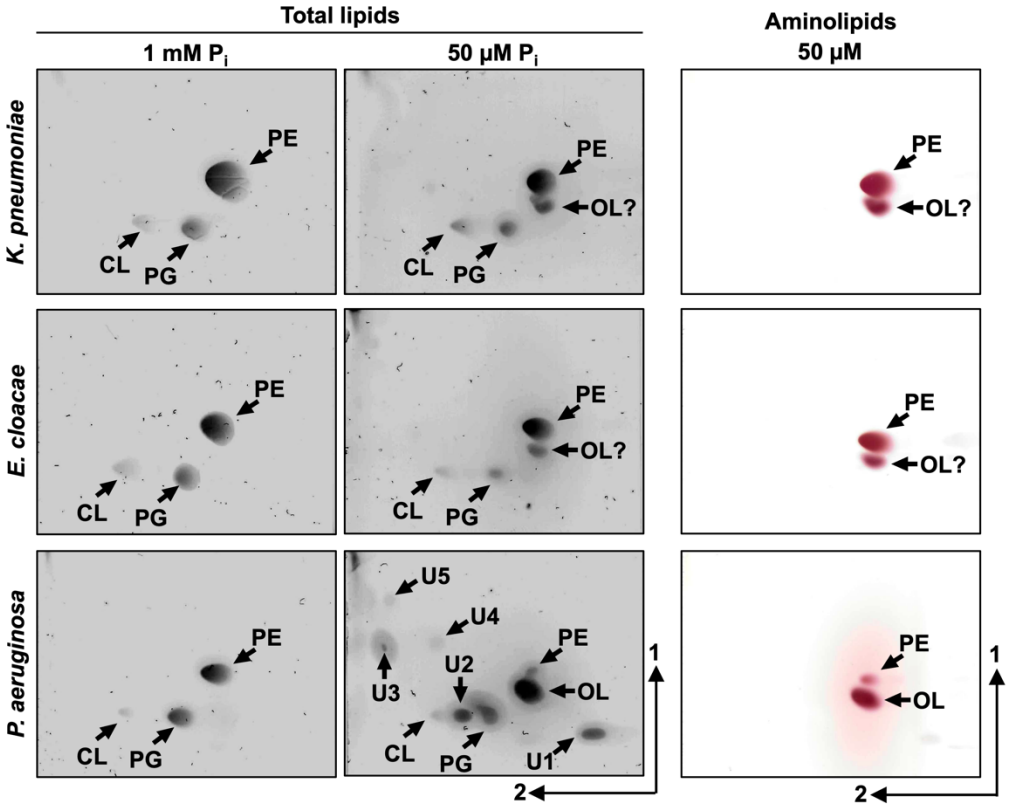

Figure 6: Aminolipid biosynthesis is conserved in Gram-negative ESKAPE pathogens. 2D thin-layer chromatography of lipids extracted from wild type *K. pneumoniae* strain KPNIH1, *E. cloacae* strain ATCC 13047, and *P. aeruginosa* strain PAO1 grown in excess (1 mM) or limiting (50 µM) phosphate conditions. Totals lipids were stained with sulfuric acid (left). Aminolipids were stained using ninhydrin (right). Specific lipids are labelled: PE, phosphatidylethanolamine; PG, phosphatidylglycerol; CL, cardiolipin; OL, ornithine lipid; U1, U2, U3, U4, and U5; unknown compounds 1, 2, 3, 4, and 5.